J Biol Inorg Chem (2008) 13:183–193
DOI 10.1007/s00775-007-0312-0

ORIGINAL PAPER

Copper incorporation into recombinant CotA laccase from *Bacillus subtilis*: characterization of fully copper loaded enzymes

Paulo Durão · Zhenjia Chen · André T. Fernandes · Peter Hildebrandt · Daniel H. Murgida · Smilja Todorovic · Manuela M. Pereira · Eduardo P. Melo · Lígia O. Martins

Received: 3 August 2007 / Accepted: 4 October 2007 / Published online: 24 October 2007

Abstract The copper content of recombinant CotA laccase from *Bacillus subtilis* produced by *Escherichia coli* cells is shown to be strongly dependent on the presence of copper and oxygen in the culture media. In copper-supplemented media, a switch from aerobic to microaerobic conditions leads to the synthesis of a recombinant holoenzyme, while the maintenance of aerobic conditions results in the synthesis of a copper-depleted population of proteins. Strikingly, cells grown under microaerobic conditions accumulate up to 80-fold more copper than aerobically grown cells. In vitro copper incorporation into apoenzymes was monitored by optical and electron paramagnetic resonance (EPR) spectroscopy. This analysis reveals that copper incorporation into CotA laccase is a sequential process, with the type 1 copper center being the first to be reconstituted, followed by the type 2 and the type 3 copper centers. The copper reconstitution of holo-CotA derivatives depleted in vitro with EDTA results in the complete recovery of the native conformation as monitored by spectroscopic, kinetic and thermal stability analysis. However, the reconstitution of copper to apo forms produced in cultures under aerobic and copper-deficient conditions resulted in incomplete recovery of biochemical properties of the holoenzyme. EPR and resonance Raman data indicate that, presumably, folding in the presence of copper is indispensable for the correct structure of the trinuclear copper-containing site.

Keywords CotA laccase · Multicopper oxidases · Copper incorporation · Copper homeostasis

Paulo Durão and Zhenjia Chen contributed equally to this work.

P. Durão · Z. Chen · A. T. Fernandes · S. Todorovic · M. M. Pereira · L. O. Martins (✉)
Instituto de Tecnologia Química e Biológica,
Universidade Nova de Lisboa,
Av. Da República,
2781-901 Oeiras, Portugal
e-mail: lmartins@itqb.unl.pt

P. Hildebrandt · D. H. Murgida
Sekr. PC14, Max-Volmer-Laboratorium für Biophysikalische Chemie,
Institut für Chemie,
Technische Universität Berlin,
Strasse des 17. Juni 135,
10623 Berlin, Germany

E. P. Melo
Centro de Biomedicina Molecular e Estrutural,
Universidade do Algarve,
Campus de Gambelas,
8005-139 Faro, Portugal

E. P. Melo
Instituto de Biotecnologia e Bioengenharia,
Centro de Engenharia Biológica e Química,
Instituto Superior Técnico,
Av. Rovisco Pais,
1049-001 Lisbon, Portugal

Introduction

Laccases are the simplest members of the multicopper oxidase (MCO) family of enzymes that includes ascorbate oxidase (L-ascorbate oxygen oxidoreductase, EC 1.10.3.3) and human ceruloplasmin [iron(II) oxygen oxidoreductase, EC 1.16.3.1]. MCOs are characterized by the presence of three types of structurally and functionally distinct Cu centers [1–3]. The type 1 (T1) Cu site is characterized by an intense $S\pi \rightarrow Cu\left(d_{x^2-y^2}\right)$ charge transfer absorption band at around 600 nm, conferring an intense blue color to these enzymes, and a narrow parallel hyperfine splitting ($A_{\|}$ =

43×10^{-4}–95×10^{-4} cm^{-1}) in the electron paramagnetic resonance (EPR) spectrum [1]. When the charge transfer excitation is used, several vibration transitions coming from Cu–S(Cys) stretching modes, centered at 400 cm^{-1}, typically appear in the resonance Raman (RR) spectra of blue copper oxidases. The intensity-weighted frequency of all these fundamental modes can provide an estimation of the Cu–S bond length and thus insight into the T1 site geometry [4]. The T1 Cu site functions in shuttling electrons from substrates to the other Cu sites. Type 2 (T2) Cu is characterized by the lack of strong absorption bands and by a larger parallel hyperfine splitting in the EPR spectrum ($A_{\|}$ = 150×10^{-4}–201×10^{-4} cm^{-1}] [1]). The type 3 (T3) or coupled binuclear Cu site is characterized by an intense absorption band at 330 nm originating from a bridging hydroxide and the lack of an EPR signal due to the antiferromagnetically coupling of the two Cu ions. Together, the T2 and T3 sites form a trinuclear center that is the site for O_2 reduction.

CotA laccase is a MCO present in the endospore coat of *Bacillus subtilis* in an active form [5]. While its exact function within the spore is still not fully understood, its assembly is essential for the full complement of spore resistance properties [6, 7]. Several recent studies have characterized biochemical and structural aspects of the CotA laccase purified from an overproducing *Escherichia coli* strain [5, 8–10]. Incomplete Cu incorporation was observed and most of the CotA laccase structures reported so far were from crystals which displayed a significant depletion of some of the Cu centers [8, 9]. Cu incorporation in MCOs is still a poorly understood process and remains an important issue of discussion in the current literature [11–15]. The understanding of this mechanism is important from biochemical, spectroscopic and structural viewpoints and also from a biotechnological perspective. In fact, laccases, owing to their high relative nonspecific oxidation capacity, find an important role in diverse biotechnological applications [16]. This work aims to gain insight into the mechanism of Cu incorporation into CotA laccase. We have identified growth conditions that allow for the production of a fully Cu loaded recombinant enzyme in the cytoplasm of *E. coli*. In addition, several spectroscopic techniques, including UV–vis, EPR and RR, as well as kinetic and thermal stability assays were used to characterize the proteins obtained through different metal-incorporation procedures.

Materials and methods

Protein recombinant production and purification

E. coli strain AH3517 [5] was grown aerobically in 1 L Luria–Bertani (LB) medium supplemented with ampicilin (100 μg mL^{-1}) in a 5-L Erlenmeyer, with 120-rpm shaking (Innova® 44, New Brunswick Scientific). The cells were grown at 30 °C until an optical density at 600 nm (OD_{600}) of 0.6 was reached, after which 0.1 mM isopropyl-β-D-thiogalactopyranoside (IPTG) and 0.25 mM $CuCl_2$ were added to the culture medium and the temperature was reduced to 25 °C. Incubation was continued for a further 4 h, when a change to microaerobic conditions was achieved by switching off the shaking function. Cells were harvested after a further 20 h of growth by centrifugation. Cell disruption and a two-step protein purification chromatographic procedure were conducted as previously described [5, 9].

Determination of cellular copper content

Aliquots of 2 mL cell culture harvested at different growth times were pelleted by centrifugation. To determine the cell dry weight pellets were dried for 16 h at 80 °C. For Cu determination, the cell pellets were washed three times with a 0.9% NaCl and 1 mM EDTA solution, resuspended in 3 mL of a mixture of 10% perchloric acid and 10% nitric acid and finally hydrolyzed at 100 °C for 1 h. The Cu content was measured by atomic absorption (Chemical Analysis Facility, Instituto Superior Técnico, Universidade Técnica de Lisboa, Lisbon, Portugal).

Preparation of apoenzyme forms

Two different forms of apoenzyme were prepared. One, apoCotA, was obtained through chromatographic purification from cells that had grown aerobically in unsupplemented-Cu LB medium [5]. A further apoenzyme was prepared by treating with EDTA [10 mM in 20 mM tris(hydroxymethyl)aminomethane–HCl buffer, pH 7.6 for 8–12 h, followed by dialysis and washing in EDTA-free buffer] a sample of CotA laccase purified from microaerobic cultures. These conditions, as discussed later, allowed the purification of an enzyme containing a full complement of Cu ions and thus we have designated this apoform as the holoCotA derivative. The Cu concentration was determined through the trichloroacetic acid/bicinchoninic acid method of Brenner and Harris [17] and confirmed by atomic absorption (Chemical Analysis Facility, Instituto Superior Técnico, Universidade Técnica de Lisboa, Lisbon, Portugal). The protein concentration was measured considering the absorption band maximum at 280 nm for CotA (ε_{280} = 84,739 M^{-1} cm^{-1}) or the Bradford assay using bovine serum albumin [18] as a standard.

In vitro copper reconstitution

For reconstitution experiments Cu was added to both apo forms of CotA laccase (see "Preparation of apoenzyme forms") either as a solution of Cu(I), obtained from stock solutions of freshly prepared $[Cu(I)(MeCN)_4]PF_6$ (Sigma-Aldrich) in argon-purged acetonitrile, or as a solution of Cu(II) ($CuCl_2$, Sigma, analytical grade). Protein samples were incubated either aerobically or anaerobically (by repeated cycles of evacuation/flushing with argon) with different molar equivalents of Cu per mole of protein for 10 min. Excess Cu was removed by repeated washing with a metal-free buffer in a Centricon unit (Amicon) before further analysis. The protein concentration and Cu content was determined as described already.

UV–vis, EPR and RR spectra and redox titration

UV–vis spectra were acquired using a Nicolet Evolution 300 spectrophotometer from Thermo Industries. EPR spectra were measured with a Bruker EMX spectrometer equipped with an Oxford Instruments ESR-900 continuous-flow helium cryostat. The spectra, obtained under nonsaturating conditions (100 μM protein content), were theoretically simulated using the Aasa and Vänngard approach [19]. Redox titrations were performed at 25 °C and pH 7.6 under an argon atmosphere, and were monitored by visible spectroscopy (300–900 nm) with a Shimadzu Multispec-1501 spectrophotometer as described by Durão et al. [10]. Back-scattered light from the frozen protein (−196 °C) was collected by a confocal spectrograph (Jobin Yvon, XY) equipped with grating of 1,800 lines per millimeter and a liquid nitrogen cooled back-illuminated CCD camera. About 2 μL of protein sample (1–2 mM) was introduced into a liquid nitrogen cooled cold finger (Linkam THMS600) mounted on a microscope stage and measured, typically with an accumulation time of 40 s, a laser power of 5 mW and binning of 1. Exciting radiation was provided by an Ar^+ 457.9 nm laser (Coherent Innova). The RR spectra (350–450-cm^{-1} region) were subjected to component analysis in which the spectra of individual modes were fitted to measured spectra. The band widths and band positions were kept constant. The fitted band intensities and frequencies were used for determination of the intensity-weighted frequency $\langle \nu_{Cu-S} \rangle$.

Activity and stability assays

Activity assays were performed as previously described [10]. Kinetic stability was performed as described by Martins et al. [5]. In brief, the enzyme was incubated at 80 °C, and at fixed time intervals samples were withdrawn and tested for activity at 37 °C using 2,2′-azinobis(3-ethylbenzthiazoline-6-sulfonic acid) (ABTS) as the substrate. Differential scanning calorimetry (DSC) was carried out in a VP-DSC instrument from MicroCal at a scan rate of 60 °C h^{-1}. The experimental calorimetric trace was obtained with 0.3 mg mL^{-1} protein at pH 3 (50 mM glycine buffer) and a baseline obtained with buffer alone was subtracted from the experimental trace. The resulting DSC trace was analyzed with the DSC software built within the Origin spreadsheet to obtain the transition excess heat capacity function (a cubic polynomial function was used to fit the shift in baseline associated with unfolding). The excess heat capacity could only be accurately fitted using a non-two-state model with three transitions (equation in the data analysis software).

Results and discussion

Growth and cell copper content

One goal of this work was to produce a recombinant, fully Cu loaded CotA laccase in the cytoplasm of *E. coli* AH 3517, in which expression of the *cotA* gene is driven upon IPTG induction of the strong T7*lac* promoter. The production of an enzymatically active laccase was shown to be dependent on the Cu supplementation of the culture media [5, 15, 20]. However, incomplete metal incorporation was observed even under these conditions [10, 15]. The existence of elaborate homeostasis mechanisms in *E. coli* (Cu-efflux and Cu-sensing systems) maintains the intracellular quota for Cu within a narrow range, owing to the well-known cytotoxicity of this transition metal [21–23]. Thus, one possibility is that overproduction of a fully Cu loaded CotA laccase is impaired by the presence of a low concentration (10 μM) of this metal in the bacterial cytoplasm [22]. Cu physiology in *E. coli* is dependent on oxygen availability, and an increased intracellular accumulation of Cu was observed under anaerobic growth conditions [24, 25]. Therefore, *E. coli* cells were grown in microaerobic conditions to promote conditions for cells to accumulate higher intracellular Cu contents. The change in the aeration conditions, from shaking (aerobic cultures) to static conditions (microaerobic cultures), in the growth course of *E. coli* AH 3517 in the presence of 0.25 mM $CuCl_2$ resulted in differences in the growth pattern and final cell yields (Fig. 1). In strictly aerobic conditions the growth reached a final OD_{600} of around 5–6. On the other hand, shortly after the promotion of microaerobic conditions, active growth was arrested and cultures reached a final OD_{600} of around 2–3. We related this observation to changes in the central metabolism of the facultative aerobe *E. coli*, since aerobic

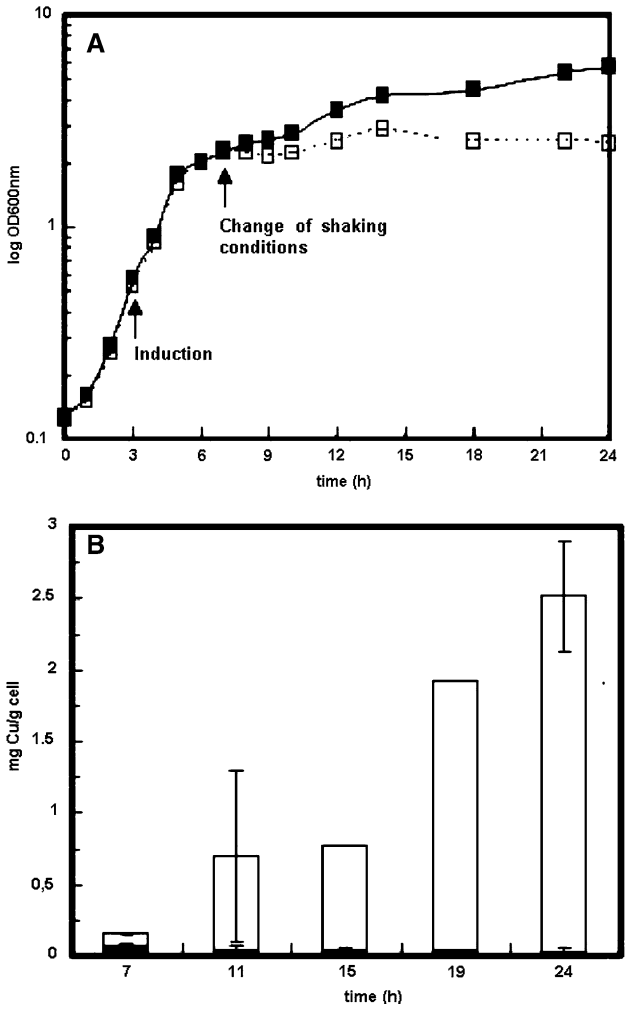

Fig. 1 **a** Growth curves of *Escherichia coli* in different aeration conditions. Exponential cells were induced at an optical density at 600 nm (*OD600nm*) of approximately 0.6 with 100 μM isopropyl-*β*-D-thiogalactopyranoside and 250 μM Cu. After a further 4 h in shaking conditions (120 rpm), cultures were exposed to shaking (*filled squares*) or static (*open squares*) conditions. **b** Intracellular Cu content of *E. coli* cells during growth under aerobic (*filled squares*) and microaerobic (*open squares*) conditions

respiration is energetically more efficient than alternative metabolic modes, as well as to the higher Cu toxicity under conditions of oxygen limitation [24, 26, 27]. Cells from microaerobic cultures showed clearly enhanced Cu content as measured by atomic absorption (Fig. 1b); these cells accumulated up to 80-fold more Cu than cells grown aerobically. The rise in Cu concentration (presumably in the more toxic cuprous form) in anaerobic conditions was related to limitations in the Cu-efflux primary Cu export system [24].

Purification and biochemical characterization

Crude extracts of *E. coli* cells grown under microaerobic conditions had twofold lower total protein content (in agreement with lower cellular yield), but remarkably a nearly 100-fold higher enzymatic activity against ABTS, when compared with crude extracts of cells grown under aerobic conditions (Table 1). Microaerobic conditions led to a reduced amount of contaminant proteins in cell extracts, allowing a higher purification yield and a lower purification factor of CotA laccase to achieve electrophoretic homogeneity (Table 1). Purified protein samples from microaerobic cultures were more intensely blue when compared with protein preparations purified from cells grown under aerobic conditions. This correlates with a stronger band intensity of the T1 Cu as monitored by the absorption at 600 nm (Fig. 2, Table 2). A shoulder at 330 nm, indicative of a hydroxyl group bridging the T3 Cu ions, was also present with an absorption intensity nearly equivalent to that of the absorption band with a maximum at 600 nm. Treatment of the protein samples with an oxidizing agent (hexachloroiridate) had no effect on the intensity of the absorption bands, showing that both enzymes were obtained in a completely oxidized state. The purified enzyme from aerobic cultures exhibited an incomplete metal incorporation (0.5:1 Cu to protein), also observed in previous studies with CotA laccase [10] (Table 2). In contrast, Cu content measurements revealed a Cu-to-protein stoichiometry close to 4 for the protein purified from cells grown under microaerobic conditions, ensuring that all four Cu ions required for enzyme activity were incorporated into the active sites. Proteins purified from cells grown under microaerobic and aerobic conditions will be subsequently referred to as holoCotA and partially Cu loaded CotA, respectively. Under microaerobic conditions cells were

Table 1 Purification of CotA laccase from *Escherichia coli* AH3517 grown under different O_2 conditions

Purification step	Protein (mg)		Total activity (μmol min^{-1})		Specific activity (μmol min^{-1} mg^{-1})		Purification factor		Yield (%)	
	Aerobic	Microaerobic	Aerobic	Microaerobic	Aerobic	Microaerobic	Aerobic	Microaerobic	Aerobic	Microaerobic
Crude extract	441	198	49.8	5,614	0.11	28.4	1	1	100	100
SP-Sepharose	25	26	34.0	5,600	1.29	219.6	11.7	7.7	96	99.8
Superdex 200	20	23	31.5	5,225	1.58	228.2	14.4	8.04	63	93

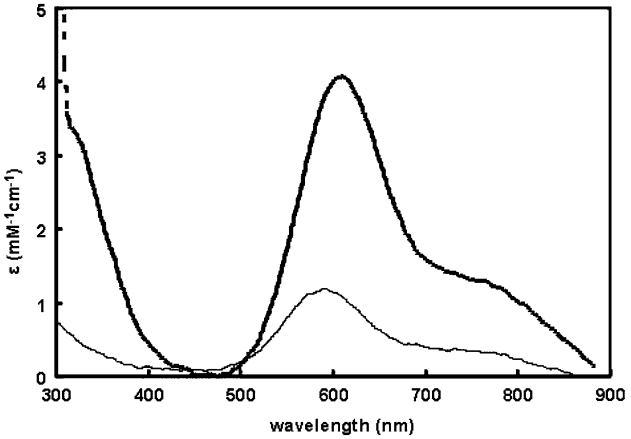

Fig. 2 UV–vis spectra of the as-isolated CotA species produced in aerobic (*thin line*) and in microaerobic (*thick line*) conditions

shown to accumulate higher amounts of Cu (see above). Although a significant portion of Cu is likely to be bound to the cell wall and other cell components, at least some of the Cu remains biologically available to the cytoplasm, possibly in the form of "metal ion pools" [22, 23], ready for incorporation into newly synthesized recombinant enzymes.

Copper incorporation into apoCotA

In order to gain a better insight into the incorporation of Cu into the CotA laccase, sample aliquots of an apoCotA purified from cells grown in unsupplemented-Cu medium were incubated with increasing molar equivalents of Cu(I) or Cu(II) and the incorporation was followed by UV–vis and EPR spectroscopies. The apoCotA had no spectral features indicative of the presence of either of the Cu sites in MCOs (Fig. 3a–c). Upon addition of one equivalent of Cu(I) a visible band with a maximum at 600 nm could be observed (Fig. 3a), demonstrating the presence of a T1 Cu site. Taking into consideration the molar absorption coefficient of the holoprotein, this accounts for approximately 40% of Cu occupancy at the T1 site. After addition of the first Cu equivalent, EPR spectral features characteristics of T1, with $g_{\|} = 2.224$, $g_{\perp} = 2.045$ and $A_{\|} = 70 \times 10^{-4}$ cm^{-1}, and T2, with $g_{\|} = 2.255$, $g_{\perp} = 2.045$ and $A_{\|} = 152 \times 10^{-4}$ cm^{-1} (Fig. 3b, c), were observed. The total paramagnetic Cu content was quantified as 1.2 per protein molecule. Occupancy of approximately 55% of Cu at the T1 site and 45% of Cu at the T2 site was determined by spectral integration. Upon the second addition of Cu the proteins contained 2 equiv of Cu. The 600 nm band increased, accounting for about 80% of Cu occupancy at the T1 site. The EPR spectra revealed the signals characteristic of T1 and T2 with 1:1 ratio, accounting for a full occupancy of both sites upon the second addition of Cu. This finding was further corroborated by the determination of the total paramagnetic Cu content, now being 2.3 per protein. This value did not change upon subsequent Cu addition. Upon further increase of the metal content, accounting for 3 equiv of Cu, the ratio between T1 and T2 is maintained but, importantly, the hyperfine constant for T2 is now larger; 174×10^{-4} cm^{-1}, reflecting a change in the Cu ligand field (Fig. 3c). Since the only difference now was the introduction of 1 equiv of Cu more, the EPR data most likely indicate the incorporation of Cu ion in the vicinity of T2, i.e., incorporation of part of the T3 site. Indeed, the 330 nm absorption band appears in the UV–vis spectra after the addition of 3 equiv of Cu, suggesting that Cu is now prevalently reconstituting the EPR-silent T3 site (Fig. 3a). Upon addition of 4 equiv of Cu neither visible nor EPR spectra show further significant changes. The results presented in this study point to a possible sequential process of Cu loading, with the T1 Cu

Table 2 Copper content and molar coefficients for different CotA forms

CotA species	Initial Cu content (mol Cu per mol protein)[a]	Final Cu content (mol Cu per mol protein)[a]	$\varepsilon_{600\ nm}$ (M^{-1} cm^{-1})	$\varepsilon_{330\ nm}$ (M^{-1} cm^{-1})
Partially Cu loaded CotA (as-isolated aerobic)	0.5 ± 0.2	–	1,300 ± 300	310 ± 138
HoloCotA (as-isolated microaerobic)	3.7 ± 0.3	–	4,075 ± 210	3,298 ± 849
ApoCotA reconstituted with Cu(II)	0.020 ± 0.001	2.5 ± 0.3	3,200 ± 200	1,691 ± 499
ApoCotA reconstituted with Cu(I)	0.020 ± 0.001	4.2 ± 0.7	3,870 ± 390	3,639 ± 815
HoloCotA treated with EDTA and reconstituted with Cu(II)	0.300 ± 0.001	4.2 ± 0.1	3,380 ± 120	4,000 ± 416
HoloCotA depleted with EDTA and reconstituted with Cu(I)	0. 300 ± 0.001	3.5 ± 0.1	3,350 ± 180	3,600 ± 107

Copper reconstitution of apoCotA or holoCotA depleted with EDTA was performed by adding 4 equiv of Cu [either Cu(I) or Cu(II)] to protein aliquots followed by dialysis and washings to remove excess Cu. Molar absorption coefficients and Cu stoichiometries were based on protein concentration determined using the absorption band maximum at 280 nm

[a] Standard errors based on errors in both Cu and protein determinations

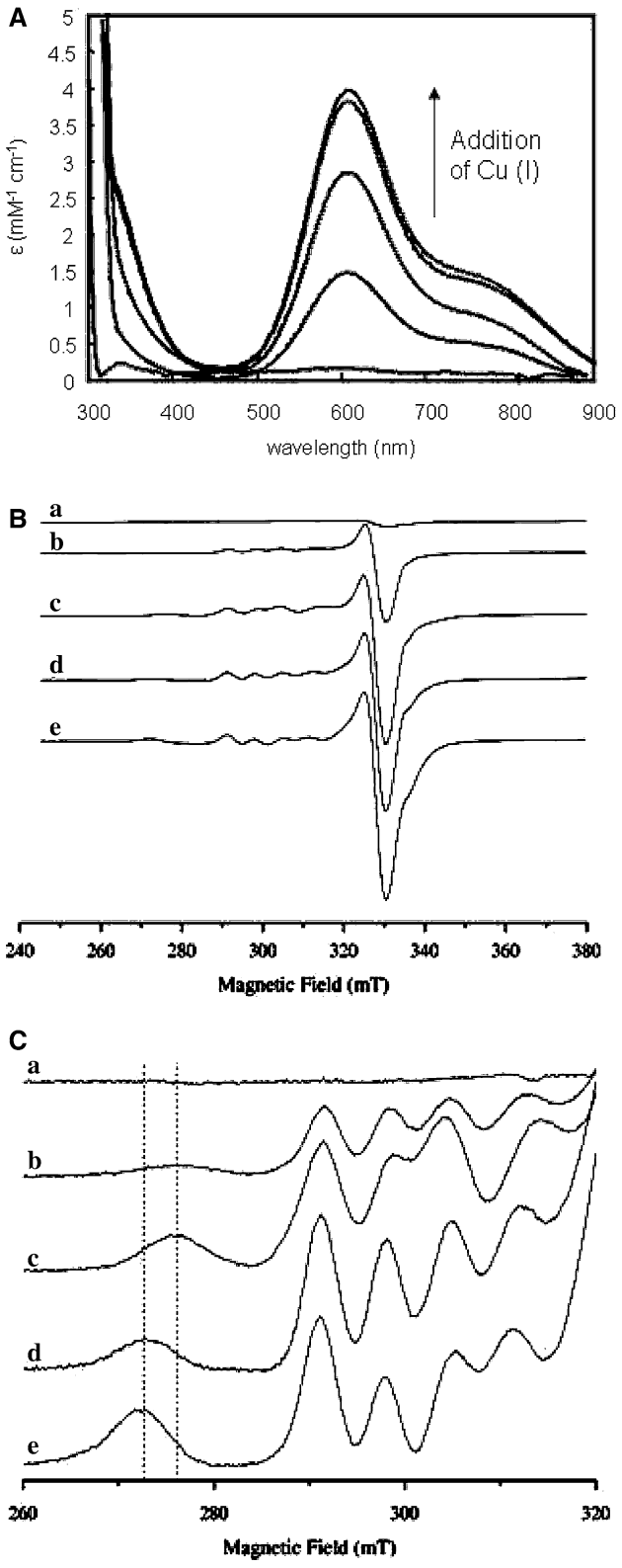

◀ **Fig. 3** Reconstitution of apoCotA with Cu(I). **a** Optical spectra, **b** EPR spectra of approximately 100 μM apoCotA before (*a*) and after sequential additions of 1 equiv (*b*), 2 equiv (*c*), 3 equiv (*d*) and 4 equiv (*e*) of Cu and **c** zoom in of **b** highlighting the differences in the hyperfine splitting constant. EPR conditions as follows: microwave frequency 9.39 GHz; microwave power 2.4 mW; modulation amplitude 0.9 mT; temperature −258 °C

center being the first to be reconstituted, followed by T2 and T3 Cu centers. Our findings are in accordance with data obtained for the MCOs CueO, Fet3p and bilirubin oxidase where partial Cu intermediates were observed [12, 15, 31]. In contrast, in human ceruloplasmin no apparent hierarchy for Cu incorporation was observed and a cooperative process of Cu loading was proposed [14].

When the incubation was performed with Cu(II), the same incorporation pattern as the one described above for the incubation with Cu(I) was observed by UV–vis and EPR spectroscopies (results not shown). However, the maximum Cu content of the protein reconstituted with Cu(II) was never higher than 2.5 Cu per protein, revealing that only a part of the total protein population becomes fully loaded. Our results clearly show that the apoCotA is reconstituted more efficiently with cuprous than with cupric ions. Although, the mechanism by which Cu centers are constructed in MCOs has not been clarified, our results suggest that recombinant CotA laccase is synthesized in the cytoplasm of *E. coli*, through incorporation of Cu(I) and not Cu(II). This is consistent with evidence that cuprous is the valence state of intracellular Cu accumulating under anaerobic conditions [24, 26]. In a similar manner, Cu incorporation of Fet3p in yeast cells was suggested to occur in the reduced form [12].

The reconstitution of the holoCotA derivatives, resulting from EDTA-depletion of the holoenzyme, followed an identical sequential incorporation pattern (results not shown). Interestingly, and in clear contrast with reconstitution of apoCotA (synthesized and folded in *E. coli* in the absence of Cu), the Cu full occupancy was reached after addition of 4 equiv of either Cu(I) or Cu(II) (Table 2). These in vitro findings show that the competent state of CotA required for Cu insertion is critically dependent of the apoenzyme preparation.

Comparative kinetic, redox potential and spectroscopic analysis

The two nonphenolic substrates, ABTS and $K_4(FeCN_6)$, and the two phenolic substrates, syringaldazine (SGZ) and 2,6-dimethoxyphenol (2,6-DMP), were used to identify specific changes in the catalytic properties of the different forms of CotA laccase obtained during this study (Table 3). Overall, the pH optima and pH profiles were similar for all enzymes tested (results not shown). No major alterations were observed regarding the K_m values for the different substrates. Significant changes were found, however, in the values of calculated k_{cat}. The

Table 3 Steady-state kinetic constants for 2,2′-azinobis(3-ethylbenzthiazoline-6-sulfonic acid) (*ABTS*), syringaldazine (*SGZ*), 2,6-dimethoxyphenol (*2,6-DMP*) and $K_4Fe(CN)_6$ for different CotA laccase forms

CotA species	ABTS		SGZ		2,6-DMP		$K_4Fe(CN)_6$	
	K_m (μM)	k_{cat} (s^{-1})	K_m (μM)	k_{cat} (s^{-1})	K_m (μM)	k_{cat} (s^{-1})	K_m (μM)	k_{cat} (s^{-1})
Partially Cu loaded CotA	101 ± 22	1.5 ± 0.2	16 ± 1	0.4 ± 0.0	358 ± 60	7 ± 1	84 ± 7	22 ± 1
HoloCotA	124 ± 17	322 ± 20	18 ± 3	80 ± 4	216 ± 35	29 ± 4	56 ± 11	529 ± 79
ApoCotA reconstituted with Cu(II)	87 ± 10	22 ± 1	10 ± 1	18 ± 0.4	273 ± 27	7.5 ± 1	69 ± 2	55 ± 1
ApoCotA reconstituted with Cu(I)	105 ± 6	82 ± 2	10 ± 2	74 ± 9	265 ± 23	16 ± 1	51 ± 5	193 ± 9
HoloCotA treated with EDTA and reconstituted with Cu(II)	126 ± 11	242 ± 15	17 ± 2	67 ± 5	192 ± 19	23 ± 1	52 ± 6	484 ± 37
HoloCotA depleted with EDTA and reconstituted with Cu(I)	134 ± 10	294 ± 15	22 ± 3	85 ± 7	202 ± 24	22 ± 1	40 ± 3	411 ± 15

Maximal activity for ABTS and $FeCN_6$ at pH 3 and for SGZ and 2,6-DMP at pH 7. The velocity data were analyzed by nonlinear fits to the Michaelis–Menten equation yielding the kinetic constants and their standard errors as shown

partially Cu loaded CotA and the holoCotA exhibited, as expected, enormous differences regarding the calculated k_{cat} values. Although the differences in the k_{cat} values are substrate-dependent, it was surprising that differences as large as 200-fold (for ABTS and SGZ oxidation) were measured. The holoCotA derivatives reconstituted with either Cu(II) or Cu(I) appear to recover the native conformation and the structure of the Cu-containing sites completely, since the k_{cat} values calculated are very close to those observed in holoCotA. The apoCotA reconstituted with Cu(II), showed 10–25% catalytic activity for the different substrates when compared with the as-isolated holoCotA. This suggests that a small fraction (10–25%) of the protein is fully loaded and redox-active, whereas the remaining incompletely loaded protein molecules do not contribute to the protein turnover. Unexpectedly, the apoCotA reconstituted with cuprous ions, exhibiting a full complement of Cu ions, has lower k_{cat} values for the oxidation of substrates compared with the as-isolated holoCotA. The difference in the turnover rates could differ as much as twofold to fivefold depending on the substrate considered.

The reduction potential of the T1 Cu site, an important factor for determining catalytic activity in MCOs, was measured for the different forms of CotA (see "Materials and methods"). The redox potential of the as-isolated holoCotA was essentially identical (525 ± 10 mV) to that of the Cu-reconstituted holoCotA derivatives. Lower redox potentials were measured for the apoCotA reconstituted with Cu(I) and with Cu(II), 498 ± 4 and 455 ± 15 mV, respectively. The measured redox potential difference (approximately 70 mV) between the holoenzymes and the apoCotA reconstituted with Cu(II), which contains 2.5 mol Cu per protein, probably reflects the heterogeneity of the sample in Cu species. These redox potential measurements correlate with the oxidation rates of the substrates tested. The as-isolated holoCotA and its reconstituted derivatives exhibited higher redox potentials and higher turnover rates than the reconstituted apoCotA. Also, the EPR spectra of the as-isolated holoCotA and the apoCotA reconstituted with Cu(I) have some differences (Fig. 4a, b). It can be observed that the T1 signal in both spectra is characterized by the same parameters, but the T2 signal is not. The g_{med} value of the latter changes significantly, which indicates some structural difference in the vicinity of the T2 center. The RR spectra of the holoCotA and the Cu(I)-reconstituted apoenzymes (both the apoCotA and the holoCotA derivatives) are essentially identical. They consist of a number of vibrational modes in the low-frequency region, originating from coupling of the Cu–S(Cys) stretch with the S–C_β–C_α(Cys) bend, as typically observed in Cu proteins containing a T1 blue Cu site [4, 29, 30] (Fig. 4c). The lower signal-to-noise ratio in the apoCotA reconstituted with Cu(I) originates from lower sample concentration. Deconvolution of the spectra (only vibrational fundamentals found below 500 cm^{-1} were considered) by component analysis reveals that all spectra can be fitted with the same spectral parameters, band frequencies and band widths. More quantitative description of the T1 site can be obtained by calculating the intensity-weighted frequency $\langle \nu_{Cu-S} \rangle$ of all Cu–S stretching modes. $\langle \nu_{Cu-S} \rangle$ is, according to Badger's law, inversely proportional to the Cu–S bond length in the T1 site [4, 28]. The intensity weighted frequency $\langle \nu_{Cu-S} \rangle$, was determined to be 410 cm^{-1} for all three enzymes, indicating the same Cu–S(Cys) bond strength. This value is within the range reported for other well-studied MCOs [4, 29, 30]. Taken together with the EPR data, the RR results indicate that different fully Cu loaded enzymes have essentially identical electronic structures on the level of the T1 Cu site, regardless of the protein preparation procedure. Nevertheless, the EPR data point to a distinct structure at the level of the T2 Cu center.

Altogether these data point to the fact that apoCotA, synthesized by *E. coli* in the absence of Cu, is unable to be reconstituted in vitro either with Cu(I) or with Cu(II) to the

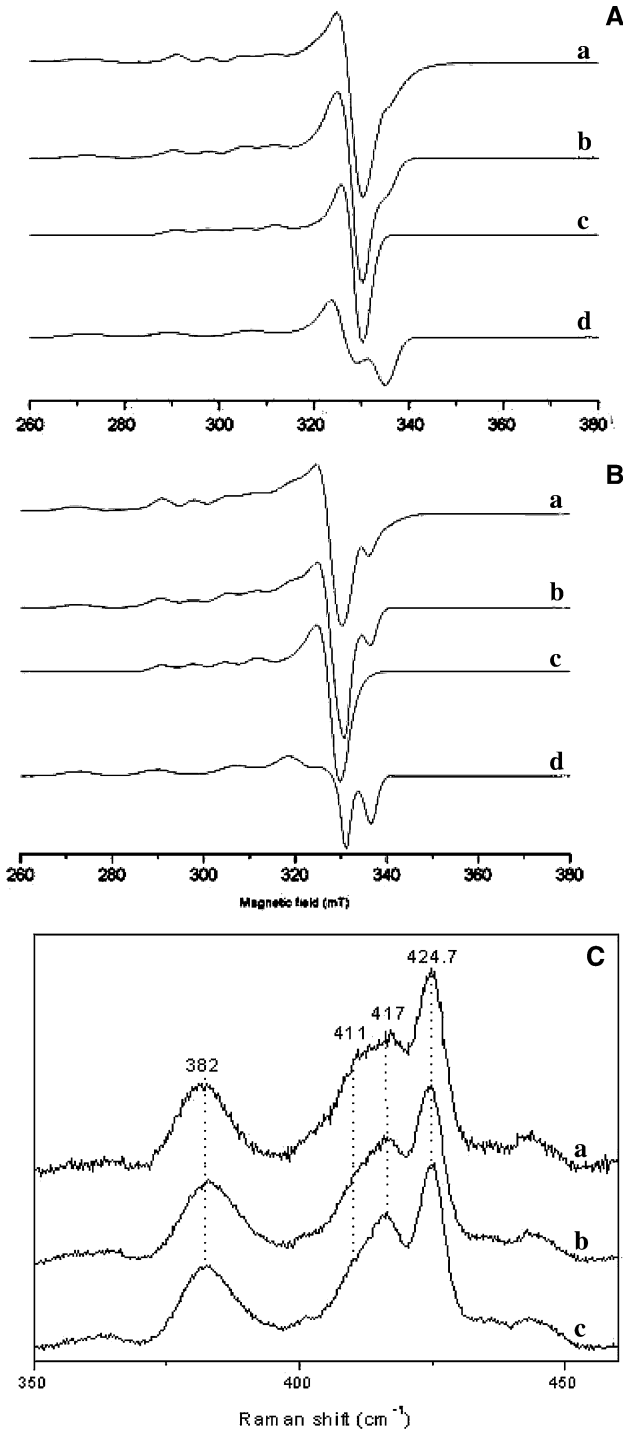

Fig. 4 **a** EPR spectra of the apoCotA incubated with 4 equiv of Cu(I) (*a*), total spectral simulation (*b*) and components (*c*, *d*). The *g* values used in simulation *b* are for type 1 $g_{min} = 2.045$, $g_{med} = 2.048$, $g_{max} = 2.229$, $A_{zz} = 71\ cm^{-1}$ and for type 2 $g_{min} = 2.033$, $g_{med} = 2.098$, $g_{max} = 2.253$, $A_{zz} = 179\ cm^{-1}$. **b** EPR spectra of the holo-CotA (*a*), total spectral simulation (*b*) and components (*c*, *d*). The *g* values used in simulation *b* are for T1 $g_{min} = 2.045$, $g_{med} = 2.048$, $g_{max} = 2.229$, $A_{zz} = 71\ cm^{-1}$ and for T2 $g_{min} = 2.040$, $g_{med} = 2.067$, $g_{max} = 2.256$, $A_{zz} = 179\ cm^{-1}$. EPR conditions as follows: microwave frequency 9.39 GHz; microwave power 2.4 mW; modulation amplitude 0.9 mT; temperature −258 °C. **c** Resonance Raman spectra of *a* 1 mM apoCotA, reconstituted with Cu(I), *b* 1.9 mM holoCotA and *c* 1.4 mM holoCotA depleted with EDTA and reconstituted with Cu(I); obtained with 567.9-nm excitation and 5-mW laser power at −196 °C, accumulation time 40 s

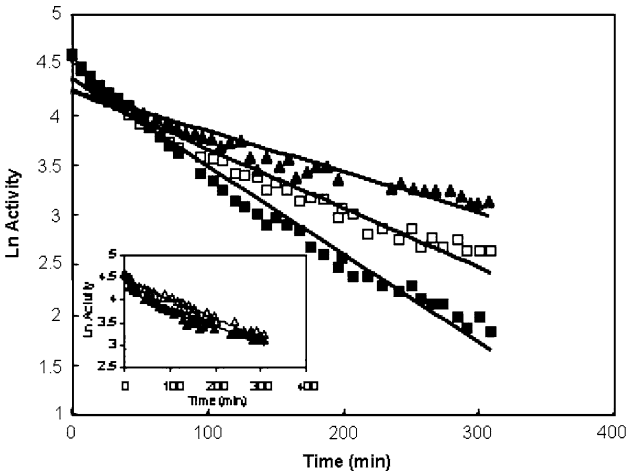

Fig. 5 Kinetic stability of the as-isolated holoCotA (*triangles*), apoCotA reconstituted with Cu(I) (*open squares*) and apoCotA reconstituted with Cu(II) (*filled squares*) at 80 °C. Deactivation obeys first-order kinetics (ln activity = ln $activity_{(t=0)} - k_d t$, where k_d is the rate constant of deactivation). The calculated half-life ($t_{1/2}$ = ln 2/k_d) for as-isolated holoCotA was 172 min ($R^2 = 0.91$), that for apoCotA reconstituted with Cu(I) was 117 min ($R^2 = 0.95$) and that for apoCotA reconstituted with Cu(II) was 79 min ($R^2 = 0.98$). The *inset* shows the comparison between deactivation of holoCotA depleted with EDTA and then reconstituted with Cu(I) which displays a half-life of 178 min (*open triangles*), and as-isolated holoCotA (*filled triangles*)

native conformation of the protein molecule. Presumably, folding in the presence of Cu is indispensable for the correct structure of the trinuclear Cu-containing site.

Thermal stability

Thermal stability was measured in order to further characterize Cu loading of the different CotA species. First, kinetic or, so-called, long-term stability was measured. Kinetic stability quantifies the amount of enzyme that loses activity irreversibly during incubation at a certain temperature (Fig. 5). Essentially, it quantifies the amount of enzyme that denatures irreversibly owing to protein aggregation, misfolding and covalent changes such as the deamidation of asparagines and the oxidation of cysteines and methionines [32]. The different species of CotA deactivate according to a first-order process, which can be described by the classical Lumry–Eyring model applied to the majority of enzymes (N ↔ U → D, where N, U and D are the native, the reversible unfolded and the irreversible denatured enzyme), pointing to a simple pathway of

unfolding and deactivation. HoloCotA is the most stable, retaining 50% of activity after 172 min at 80 °C. Although apoCotA reconstituted with Cu(I) contains roughly the same Cu content as holoCotA, it is less stable, having a half-life of 117 min. The least stable species is apoCotA reconstituted with Cu(II), containing 2.5 Cu per protein, which takes 79 min to lose 50% of its initial activity. The reconstituted holoCotA derivatives [reconstituted with either Cu(I) or Cu(II)] have a half-life of 178 min and are therefore as stable as holoCotA.

The thermal stability of different CotA species was also probed by DSC to gather additional insight into the specificity of Cu incorporation, through its effect on protein stability. DSC gives unique information on the thermal stability of proteins based on heat changes, besides the measurement of protein unfolding temperatures. The DSC thermogram reveals a complex process for two reasons (Fig. 6). Firstly, aggregation after unfolding was observed even at pH 3, leading to 100% irreversibility (no peak in the second scan). Secondly, the excess heat capacity can only be fitted by considering three independent transitions. Three thermal transitions were previously used to describe DSC traces of ascorbate oxidase [33] and ceruloplasmin [34]. Interestingly, the temperature at the mid-point of each transition clearly reflects the stability of each species of CotA (T_m values in Fig. 6). The as-isolated holoCotA is around 2 °C more stable than the apoCotA reconstituted with Cu(I), independently of the transition under consideration. This latter species is in turn more stable than the apoCotA reconstituted with Cu(II), but the differences in T_m values depend on the transition, being 7.1, 4.6 and 3.6 °C for the first, second and third transition, respectively. The reconstituted holoenzyme derivatives [reconstituted either with Cu(I) or with Cu(II)] are even slightly more stable than the holoCotA (T_m values in parentheses in Fig. 6, scan A). In addition, each transition measured by DSC is a non-two-state process as the calorimetric molar enthalpy is significantly smaller than the van't Hoff enthalpy. The behavior is similar for the three species of CotA, with the ratio $\Delta H_{cal}/\Delta H_{vH}$ taking the values of 0.94, 0.52 and 0.18 for the first, second and third transition of as-isolated holoCotA, respectively. Ratios $\Delta H_{cal}/\Delta H_{vH}$ smaller than 1 indicate protein aggregation [35] and explain why thermal unfolding of CotA leads to irreversibility even at pH 3.

Interestingly, both kinetic and thermal stability data for the different Cu-loaded forms of CotA reflect a clear pattern. HoloCotA is the most stable, followed by apoCotA reconstituted with Cu(I), and the least stable is apoCotA reconstituted with Cu(II). These results show that Cu content as well as Cu incorporation (in vivo vs. in vitro) have a direct impact on the stability of the enzyme. If holoCotA is depleted with EDTA and then reconstituted with Cu, it becomes as stable as the original species, meaning that the protein fold acquired in vivo and the Cu coordination are crucial for maximum stability. Cu binding to MCOs is well known to stabilize the enzyme [36, 37] and indeed we have observed this stabilizing effect both for kinetic and for thermal stability. Stabilization by Cu

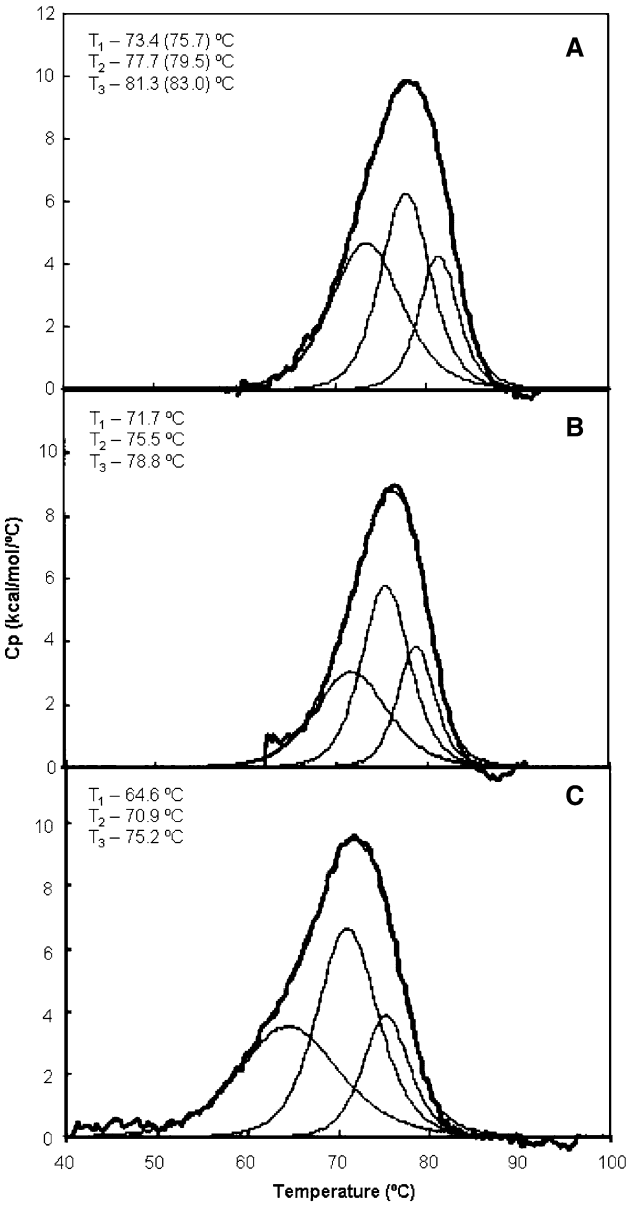

Fig. 6 Excess heat capacity obtained from a differential scanning calorimetry (DSC) scan (at pH 3) of as-isolated holoCotA (*A*), apoCotA reconstituted with Cu(I) (*B*) and apoCotA reconstituted with Cu(II) (*C*). The *thick line* (experimental data) was fitted with three independent transitions shown separately in *thin lines*. The *thin line* under the DSC trace is the resulting sum of the three independent transitions. T_m values for the three transitions are shown, with the T_m values in *parentheses* referring to the holoCotA depleted with EDTA and then reconstituted with Cu(I). The standard deviation of T_m is between 0.6 and 2.3 °C

depends on the type of coordination involved (T1, T2 or T3) [36, 38, 39] but probably also on subtle changes of each coordination geometry, as pointed out by the differences in stability between apoCotA reconstituted with Cu(I) and the as-isolated holoCotA and its reconstituted derivatives which have the same Cu content.

Concluding remarks

In this study we have described the procedure for obtaining a soluble recombinant bacterial laccase with its full complement of Cu ions from *E. coli*. We have shown that Cu physiology is dependent on the oxygen availability; under microaerobic growth conditions in Cu-supplemented media, cells accumulate higher amounts of Cu than when grown under aerobic conditions. Microaerobically grown cells are able to produce, in the cytoplasmic space, a recombinant holoCotA enzyme, while in aerobic conditions a Cu-depleted population of proteins becomes expressed. Possibly, the heterologous expression of a fully Cu loaded enzyme under aerobic conditions by *E. coli* is impaired by the presence of low cellular concentrations of this transition metal ion. Visible and EPR data point to a sequential process of Cu loading, with the T1 Cu center being the first center to be reconstituted, followed by the T2 Cu and T3 Cu centers. The sequential reconstitution with cuprous or cupric ions of apoCotA, synthesized by *E. coli* in the presence of oxygen in unsupplemented-Cu media, showed that a fully Cu loaded reconstituted enzyme is obtained only when the incorporation occurs in the presence of Cu(I). These observations suggest that the CotA laccase is synthesized in vivo through incorporation of the +1 oxidation state. Nevertheless, the apoCotA reconstituted with Cu(I), even with its full complement of Cu ions, possesses lower catalytic ability and thermal stability when compared with the as-isolated holoCotA. These results point to a critical role of Cu in the correct folding of recombinant CotA laccase in the cytoplasm of *E. coli*. In fact, the reconstitution with either cuprous or cupric ions of holoCotA derivatives obtained in vitro by treatment with EDTA completely recovers the properties of the native enzyme. EPR and RR data of the holoCotA and the Cu(I)-reconstituted apoenzymes (both the apoCotA and the holoCotA derivatives) presented essentially identical electronic structures on the level of the T1 Cu site. The EPR data indicate some structural difference in the vicinity of the T2 center. Taken together the EPR and RR data indicate that, presumably, folding in the presence of Cu is indispensable for the correct structure of the trinuclear Cu-containing site, and could partly explain the differences in the kinetic and stability properties of the enzymes.

Acknowledgements This work was supported by POCI/BIO/57083/2004 and FP6-2004-NMP-NI-4/026456 project grants. P.F. Lindley and A. Sanchez Amat are acknowledged for their useful suggestions. We thank P. Jackson for correcting the English. Z. Chen holds a Post-doc fellowship (SFRH/BPD/27104/2006) and A.T. Fernandes a PhD fellowship (SFRH/BPD/31444/2006).

References

1. Solomon EI, Sundaram UM, Machonkin TE (1996) Chem Rev 96:2563–2605
2. Stoj CS, Kosman DJ (2005) In: King RB (ed) Encyclopedia of inorganic chemistry, vol II, 2nd edn. Wiley, New York, pp 1134–1159
3. Lindley PF (2001) In: Bertini I, Sigel A, Sigel H (eds) Handbook on metalloproteins. Dekker, New York, pp 763–811
4. Blair DF, Campbell GW, Schoonover JR, Chan SI, Gray HB, Malmstrom BG, Pecht I, Swanson BI, Wooddruff WH, Cho WK, English AM, Fry HA, Lum V, Norton KA (1985) J Am Chem Soc 107:5755–5766
5. Martins LO, Soares CM, Pereira MM, Teixeira M, Jones GH, Henriques AO (2002) J Biol Chem 277:18849–18859
6. Hullo M-F, Moszer I, Danchin A, Martin-Verstraete I (2001) J Bacteriol 183:5426–5430
7. Donovan W, Zheng L, Sandman K, Losick R (1987) J Mol Biol 196:1–10
8. Enguita FJ, Martins LO, Henriques AO, Carrondo MA (2003) J Biol Chem 278:19416–25
9. Bento I, Martins LO, Gato GL, Carrondo MA, Lindley PF (2005) Dalton Trans 21:3507– 3513
10. Durão P, Bento I, Fernandes AT, Melo EP, Lindley PF, Martins LO (2006) J Biol Inorg Chem 11:514–526
11. Davis-Kaplan SR, Askwith CC, Bengtzen AC, Radisky D, Kaplan J (1998) Proc Natl Acad Sci USA 95:13641–13645
12. Blackburn NJ, Ralle M, Hassett R, Kosman DJ (2000) Biochemistry 39:2316–2324
13. Palmer AE, Szilagyi RK, Cherry JR, Jones A, Xu F, Solomon EI (2003) Inorg Chem 42:4006–4017
14. Hellman NE, Kono S, Mancini GM, Hoogeboom AJ, de Jong GJ, Gitlin JD (2002) J Biol Chem 277:46632–46638
15. Galli I, Musci G, di Patti MCB (2004) J Biol Inorg Chem 9:90–95
16. Xu F (1999) In: Flickinger MC, Drewn SW (eds) Encyclopedia of bioprocess technology: fermentation, biocatalysis and bioseparation. Wiley, New York, pp 1545–1554
17. Brenner AJ, Harris ED (1995) Anal Biochem 226:80–84
18. Bradford MM (1976) Anal Biochem 72:248–254
19. Aasa R, Väangard VT (1975) J Magnet Reson 19:308–315
20. Sanchez-Amat A, Lucas-Elio P, Fernández E, Garcia-Borrón JC, Solano F (2001) Biochim Biophys Acta 1547:104–116
21. Grass G, Rensing C (2003) FEMS Microbiol Rev 27:197–213
22. Changela A, Chen K, Xue Y, Holschen J, Outten CE, O'Halloran TV, Mondragón A (2003) Science 301:1383–1387
23. Finney LA, O'Halloran TV (2003) Science 300:931–936
24. Outten FW, Huffman DL, Hale JA, O'Halloran TV (2001) J Biol Chem 276:30670–30677
25. Macomber L, Rensing C, Imlay JA (2007) J Bacterial 189:1616–1626
26. Beswick PH, Hall GH, Hook AJ, Little K, McBride DCH, Lott KAK (1976) Chem Biol Interact 14:347–356
27. Partdridge JD, Sanguinetti G, Dibden D, Roberts RE, Poole RK, Green J (2007) J Biol Chem 282:11230–11237
28. Green MT (2006) J Am Chem Soc 128:1902–1906
29. Palmer AE, Randall DW, Xu F, Solomon EI (1999) J Am Chem Soc 121:7138–7149

30. Machokin TE, Quintanar L, Palmer AE, Hassett R, Severance S, Kosman DJ, Solomon EI (2001) J Am Chem Soc 123:5507–5517
31. Kataoka K, Kitagawa R, Inoue M, Naruse D, Sakurai T, Huang H-W (2005) Biochemistry 44:7004–7012
32. Volkin DB, Klibanov AM (1989) In: Creighton TE (ed) Minimizing protein inactivation protein function. A practical approach. IRL, Oxford, pp 1–24
33. Savini I, D'Alessio S, Giartosio A, Morpurgo L, Avigliano L (1990) Eur J Biochem 190:491–495
34. di Patti MCB, Musci G, Giartosio A, D'Alessio S, Calabrese L (1990) J Biol Chem 265:21016–21022
35. Vassall KA, Stathopulos PB, Rumfeldt JAO, Lepock JR, Meiering EM (2006) Biochemistry 45:7366–7379
36. Agostinelli E, Cervoni L, Giartosio A, Morpurgo L (1995) Biochem J 306:697–702
37. Ragusa S, Cambria MT, Pierfederici F, Scirè A, Bertoli E, Tanfani F, Cambria A (2002) Biochim Biophys Acta 1601:155–162
38. Koroleva OV, Stepanova EV, Binukov VI, Timofeev VP, Pfeil W (2001) Biochimic Biophys Acta 1547:397–407
39. Milardi D, Grasso DM, Verbeet MP, Canters GW, La Rosa C (2003) Arch Biochem Biophys 414:121–127